A CONCEPTUAL DESIGN AND ANALYSIS TOOL FOR BLENDED WING BODY AIRCRAFT

Jorrit van Dommelen and Roelof Vos
Delft University of Technology, 2600GB Delft, The Netherlands

Keywords: *Blended Wing Body, Conceptual Design, Design Engine*

Abstract

Due to the unconventional nature of the blended wing body (BWB) no off-the shelf software package exist for its conceptual design. The present paper details a first step towards the implementation of traditional and BWB-specific design and analysis methods into a software tool to enable preliminary sizing of a BWB. The tool is able to generate and analyze different BWB configurations. The present paper discusses the results of three different configurations. The first configuration is an aft-swept BWB with aft mounted engines, the second configuration is an aft-swept BWB with wing mounted engines and the third configuration is a BWB with forward swept BWB with wing mounted engines. These aircraft comply with the same set of top-level requirements and airworthiness requirements.

1 Introduction

Since the introduction of the tube-and-wing (TAW) jetliners in the late 1950s, their range parameter, $M_{\text{cruise}} \times L/D$, has been steadily increasing from 13 in 1960 to 16 in the mid 1990s.[1] Because designers of TAW aircraft can rely on realistic solutions from decades of research into this configuration, it is unlikely that significant gains can be achieved unless radically new technologies are employed. There are various alternative concepts proposed to the TAW configuration. One of those concepts is the blended-wing-body (BWB) configuration, which consistently promises to increase the aerodynamic efficiency by another 25%[2,3] and is the only nonconventional concept that airline manufacturers have taken an interest in (notably Boeing's 8.5%-scale BWB demonstrator). Although, on a first glance, the 25% increase might not seem as revolutionary, it does when one realizes that it took more than 45 years to achieve this improvement on a conventional TAW jetliner.

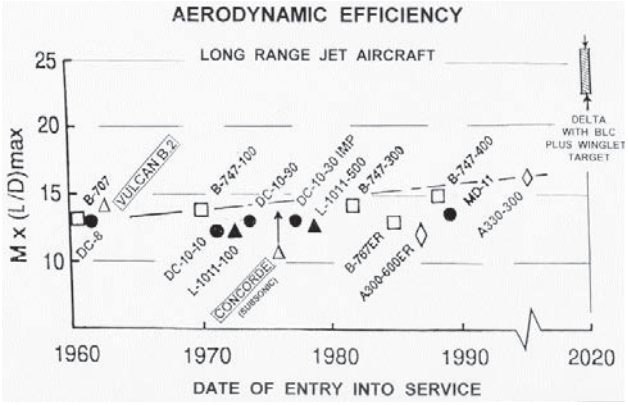

Fig. 1 Aerodynamic Efficiency - $(M_0 \times L/D)$ variation with date of entry into service[1]

For TAW aircraft, there are sufficient airplane design handbook methods available to perform conceptual design studies. Several off-the-shelf software packages can be used that have these methods integrated in a user-friendly computer code (e.g. Advanced Aircraft Analysis (AAA) by DARcorp or Program for Aircraft Synthesis Studies (PASS) by Desktop Aeronautics). However, due to the unconventional nature of the blended wing body there exists no such tool for their conceptual design based on a given set of

top level requirements. The present paper details a first step towards the implementation of traditional and BWB-specific design methods into a software tool that aids the designer in the conceptual design of a BWB aircraft.

2 Structure of the Design and Analysis Program

All calculations are performed from the MATLAB environment, using customary written calculation modules, centered around a main module. For a detailed description of each of the modules the reader is referred to Van Dommelen, 2011.[4] The present paper summarizes the design and analysis modules and discusses exemplary the results. The program automatically designs a single BWB aircraft for a given set of input parameters and analyzes several key characteristics. The program structure is solely based on a feed-forward structure and is presented in Figure 2.

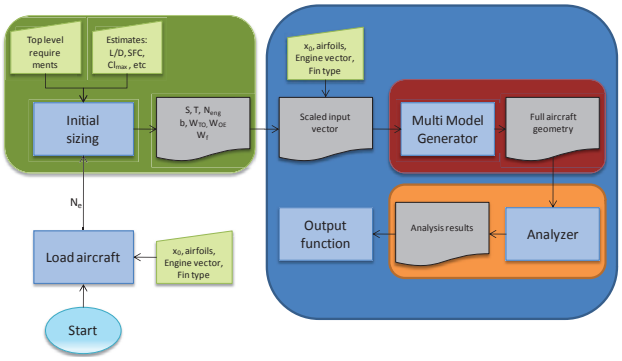

Fig. 2 Single aircraft calculation structure and blocks

When the program is started, the configuration of the aircraft has to be defined by the user. The input consists of four vectors. The first vector describes the shape of the planform and the vertical tail. The second vector is the airfoil vector, which defines the airfoils used at various spanwise locations as defined in streamwise direction. The third vector defines the number of engines and their location. There are two options for the engine location: body mounted engines and wing mounted engines. The final vector describes the vertical tail configuration. There are four options for the vertical tail type. The first option is a single body mounted vertical tail. The second option is a twin tail at the trailing edge of the centerbody. The third option is the winglet option, which means that the vertical tail planes are fixed at the wing tips of the aircraft. The final option is to use no vertical tail at all.

The first part of the program is the initial sizing, indicated in green in Figure 2. Here the wing loading, thrust-to-weight ratio is calculated based on the method laid out in Roskam, 2005[5] and data from conventional aircraft as well as estimated blended wing body data based on literature. After the initial sizing the program constructs discipline specific models of the aircraft in the multi-model generator module of the program. The models are subsequently used to analyze the aircraft on various disciplines, see Section 2.3. The output module post-processes the data and generates a variety of plots. Each of these modules are described in more detail in the next sections.

2.1 Preliminary Sizing Module

Preliminary sizing of thrust and wing loading as well as a Class I weight estimation are carried out according to traditional handbook methods.[6] Estimates of BWB aircraft from previous studies[2,3,7] are taken into account along with conventional aircraft data where necessary. For a given set of range requirements and assumptions on aerodynamic and engine performance, this module calculates the take-off weight, fuel weight, and operational empty weight of the airplane. With appropriate choices, based on prior research into BWB aircraft, for the design maximum lift coefficients and wing aspect ratio, the design point in the the thrust loading vs. wing loading diagram is calculated. The design point determines the take-off thrust and the wing area. Through the aspect ratio, the wing span is also fixed. The input vector describing the planform of the aircraft is scaled to match the wing area and wing span estimations of the initial sizing. This approach is used to increase the probability

to arrive at a feasible aircraft design at the end of the conceptual design phase.

2.2 Multi Model Generator Module

The multi model generator (MMG) uses the output from the preliminary sizing along with specified user input on the wing geometry, the selected airfoils, the engine configuration and the vertical tail configuration to generate the following models:

- geometric model of the outer shell including disposition of vertical tail and engines
- model of the interior volume: passenger cabin, cargo space and fuel tank
- structural disposition of the wing box
- vortex lattice model of the wing planform

Figure 3 displays all data generated by the model generator. This data is used in the analysis modules of the program.

2.2.1 Geometric Model of the Outer Shell

The geometric model of the outer shell consists of three parts: the aerodynamic surface of the wing-body combination, the vertical tail surfaces and the engines. The multi model generator starts by generating the aerodynamic surface of the wing-body combination. This surface is formed by reading the scaled input vector. The wing-body surface is divided in several trunks. The shape is described by the root chord and five additional parameters per wing trunk, displayed in Table 1.

Input	Variable	Symbol
Wing input	Root chord	c_1
Input per trunk	Trunk's tip chord	c_{n+1}
	Trunk's tip span	b_{n+1}
	Twist at c_{n+1}	ε_n
	Sweep trunk n	Λ_n
	Dihedral trunk n	Γ_n

Table 1 Wing-body input parameters

The planform is formed by defining the 2D planform and subsequently adding dihedral and twist. The aerodynamic surface is formed by a lofting process. The airfoil at each trunk end is defined in the input vector. By interpolating the airfoils, the aerodynamic surface of the BWB is formed.

The definition of the vertical tail is similar to the wing-body definition. Two additional input parameters are needed to fix the location of the vertical tail. These are the y-position with respect to the centerline and the distance from the leading edge. The tail is automatically fixed to body in z-direction by the multi-model generator. Generally speaking, only a single trunk is needed to describe the vertical tail. Not all vertical tail input parameters are used for certain tail configurations. An example is a winglet configuration. In that case, the tail root chord is set equal to the wing tip chord.

The airfoils used for the wing-body are based on the whitcomb supercritical airfoil. The camber is removed, while the thickness distribution is preserved. The thickness is controlled by the input vector. The vertical tail airfoils are symmetric NACA 4-series profiles with a thickness of 14% at the root and 12% at the tip.

The final part of the outer shell is formed by the engines. Two options for the engine positions are considered. The engines can be placed at the aft-body or beneath the wings. The position and number of engines is described by the engine input vector. The multi-model generator finds the exact location of the engine by considering the aerodynamic surface of the wing-body and the location of the vertical tail.

2.2.2 Cabin and Fuel Volume

The internal model consists of the fuel tanks and the pressure cabin. The fuel tanks are located in the outer trunks of the wing. In this study the fuel tanks are assigned to the two outboard wing trunks. The fuel tanks are located inside the torsion box and extend to 85% of the semi wing span.

The pressure cabin is formed by a separate

structure, which has to withstand pressurization loads. Liebeck[2] proposed two concepts for the pressurized cabin for BWB. One with an integrated skin and pressure shell. This requires a thick sandwich structure for both the upper and lower wing surfaces, which takes both aerodynamic loads and pressurization loads. A second approach is a separate pressurization structure, which carries only pressurization loads. This pressure vessel is thin-walled and is loaded solely in tension. The latter approach is used in this study. This structures takes the form of a multi-bubble structure. By using a separate structure, the functions of the aerodynamic structure and the cabin are separated. the multi-model generator determines the geometry of the multi bubble pressure cabin. The structure consists of straight cylinders, which are joined together.

2.2.3 Structural Model of the Wing-Body

The third model created by the multi model generator is a structural model of the wing-body combination. This model forms the basic shape of the wingbox, which carries the loads through the structure. The front and rear spar are assumed to be located at fixed chord percentages at 13% and 72%, respectively. This model is used for the Class II weight estimation. The weight of the wing-body structure is determined by considering the wingbox as the load carrying structure which is statically determined.

2.2.4 Vortex Lattice Model

The multi model generator generates a program specific model for the aerodynamic analysis module. A vortex lattice method is employed. The aircraft consist of the wing-body and the vertical tail surfaces and is modeled with zero thickness. This model is used for the calculation of the lift and drag polar in cruise flight along with stability derivatives.

2.3 Analysis Module

After the full geometry of the aircraft is generated, a set of modules analyzes key characteristics of the airplane. The first module is the payload module, which uses the cabin layout to analyze the volume and area available for the passenger cabin and the cargo bays. The second module performs a basic aerodynamic analysis based on a vortex lattice method. When the aerodynamic loads are known, a detailed (Class II) weight estimation is performed and the center of gravity (CG) travel during loading and flight is determined. The landing gear position and strut lengths are calculated based on the CG range, clearance and loading requirements. Combining the CG and aerodynamic information, the trim deflection in cruise flight is estimated along with estimates for the trim drag. In addition, estimates are made for the static longitudinal, directional and lateral stability, take-off rotation capability and OEI controllability. Subsequently, the performance module calculates the payload-range diagram and estimates the take-off field length, the landing length, and the attainable climb gradients for various engine operating/non-operating conditions. The final module compares the output from each of the analysis modules to the top-level requirements and aviation regulations. This analysis block is visualized in Figure 4 and discussed in detail below.

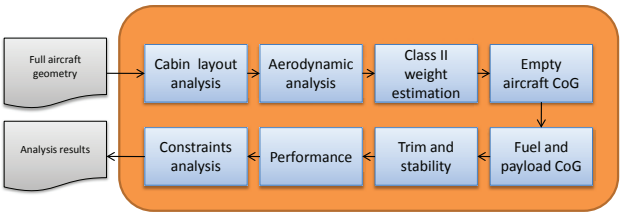

Fig. 4 Analysis block flow diagram

2.3.1 Payload Module

The payload module analyzes the pressure cabin generated by the multi model generator. The required amount of passenger cabin floor area and the required cargo volume are determined from the top-level requirements. The payload module determines the location of the passenger cabin floor, see Figure 5.

Subsequently, the payload module calculates the available floor area and cargo volume. The

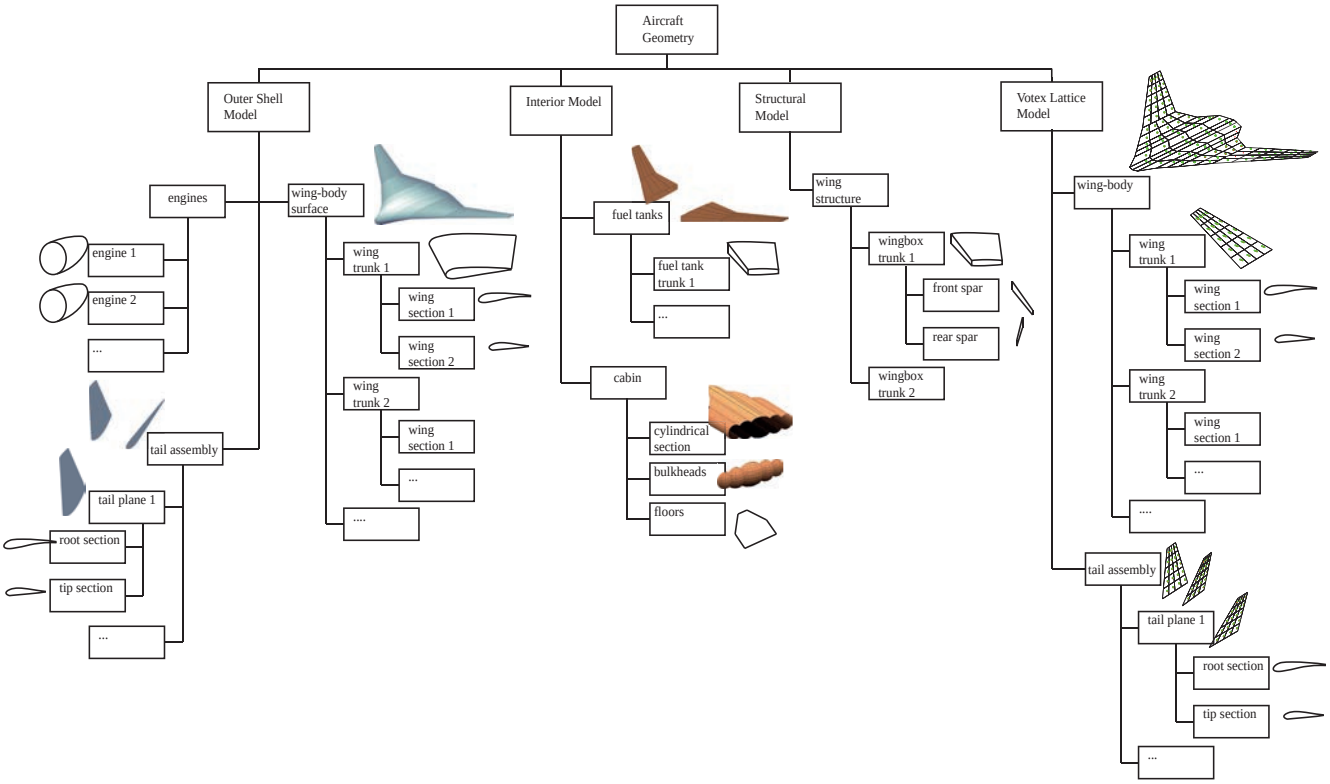

Fig. 3 Graphical overview of data generated by the MMG

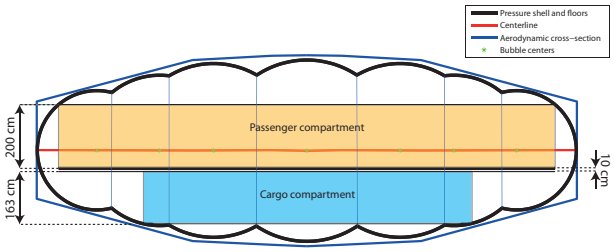

Fig. 5 Cross-section of the cabin, showing passenger and cargo compartments

vertical dimension of 1.63m is considered to calculate the available cargo volume, to give the possibility to accommodate the most common LD type cargo containers and pallets.

2.3.2 Aerodynamic Module

The second analysis module is the aerodynamic module. The aerodynamic module uses the vortex lattice method to determine the lift polar for cruise conditions. The determination of the induced drag is done using a Trefftz plane analysis. For the determination of the zero-lift drag, the method of Raymer is used.[8] This method uses the flat-plate friction drag and form factors to estimate the zero-lift drag.

Secondly, the aerodynamic module estimates the maximum lift coefficient. First the maximum lift coefficient in clean configuration is determined. This is done by taking the sections' maximum lift coefficient into account. These values are determined from experimental data.[9] The spanwise lift distribution is interpolated until the sections' maximum lift coefficient is reached. The corresponding lift coefficient is considered to be the maximum lift coefficient of the aircraft. The effect of the addition of slats, which are assumed to be the only high-lift devices present, is determined from handbook methods.

The final part of the aerodynamic module is to estimate the critical Mach number and the Drag Divergence Mach number. These values are used to conclude if the design is considered feasible. The relation between quarter chord sweep,

local thickness and lift coefficient from Kroo[10] is used to estimate the critical Mach number. The drag divergence Mach number is estimated by adding 0.05 to the critical Mach number.

2.3.3 Weight Module

With the aerodynamic parameters estimated, a second, more detailed weight estimation is performed. This weight estimation is based on the actual dimensions of the aircraft, whereas the Class I weight estimation was solely based on statistical and empirical relations.

The take-off weight is kept constant to the take-off weight calculated in the initial sizing, as is the payload weight. This means that empty weight is traded for fuel weight. This approach means that no iterations in design weight are required.

Traditionally, empirical relations between the aircraft dimensions and components weight are used in Class II weight estimation. This is sufficiently accurate for conventional aircraft, but cannot be applied to the structural components of unconventional aircraft. The primary structural component is the wing-body structure. The weight is estimated using the method of Torenbeek.[11] This method assumes that all loads will be ultimately concentrated in the primary wingbox structure, consisting of upper and lower stiffened panels, a front and rear spar and ribs. The method assumes that the wingbox is statically determined, where bending forces are absorbed by the stiffened skin panels and shear forces are transferred by the spar webs. Torsional loads are not taken explicitly into account. Maneuvering and gust loads are considered as the determining load cases. Correction factors are applied to the idealized structure to account for non-tapered skins, splices, joints and access panels. The wing box weight is determined per wing trunk, using the structural model of the wing-body as generated by the multi-model generator. The bending moment and shear forces are calculated from the lift distribution, which is determined in the aerodynamic module. The weight of the secondary wing-body structure, the empirical relations from Torenbeek[11] are used.

The pressure cabin forms a separate structure, which is assumed to absorb the load caused by the pressure difference only. When using a multi-bubble structure as described by Geuskens *et al.*,[12] the structural weight is independent of the shape. A Correction factor of 2 is applied to account for the absence of continuous vertical walls between the bubbles of the structure. A second correction is applied for the existence of doors in the structure according to Raymer.[8]

The weight of the vertical tail and the weight of the aircraft's systems is determined using the method of Raymer.[8] The use of this method is possible since the systems do not differ fundamentally from conventional aircraft.

2.3.4 Center of Gravity Module

With the aircraft component's weight known, the program determines the center of gravity of the empty aircraft. The geometrical model is used to estimate the position of the components.

The center of gravity at each point in flight depends on the amount of payload, the amount of fuel and the way the fuel is loaded. These loading conditions are taken into account by dividing the payload-range diagram in 31 points. Each of these points on the horizontal axis is considered to be a missions. Each mission is divided in 109 phases. For the flight phases other than the cruise flight, fixed fuel fractions are used. The remaining fuel fraction for the cruise phase is divided in 100 phases. A total of 4 different fuel loading schemes are considered. The fuel tanks are located in the two outboard wing trunks. Loading combinations are formed by filling either the inboard or the outboard tank completely, and start using the fuel from either one of these fuel tanks first. The center of gravity is calculated for each of these situations and is stored in a 31x109x4 matrix.

Based on the center of gravity range occurring in ground operations, the landing gear position is determined. The rules as described by Raymer[8] are used. Based on the clearance margins of the aft end of the body, the engines and

the wing tips, the length of the landing gear is determined.

2.3.5 Trim and Stability Module

The trim and stability module starts by determining the trim position for each center of gravity case. To be trimmed in longitudinal direction, the lift must equal the drag and the aerodynamic moment must equal the moment generated by the aircraft's weight. This creates a system of two equations, which can be solved to determine the trim deflection of the pitch control surfaces and the angle of attack. The aerodynamic derivatives as determined by the aerodynamic module are used. Using the angle of attack and the trim deflection, the trim drag is estimated. The trim drag is found by considering the derivative of C_{D_δ} with respect to α. Multiplying this derivative by the trim deflection δ and the angle of attack α, gives an indication for the increase in drag coefficient due to the elevator deflection.

The static longitudinal stability is determined by calculating the minimum static margin. The static margin is the difference between the center of gravity position and the neutral point. The neutral point is found by dividing the difference in aerodynamic moment for two different angles of attack, by the difference in lift coefficient at these angles of attack. These moments are already known from the aerodynamic module. The minimum static margin is determined by considering the distance between the most aft center of gravity position and the neutral point, expressed in terms of the mean aerodynamic chord (MAC). In the present study some instability is allowed: the minimum static margin is set at -10%.

The directional and lateral stability are taken into account by considering the weathercock stability and the rolling moment due to sideslip, respectively. The coefficients are obtained from the aerodynamic module, with a correction for the absence of thickness in the vortex lattice model. Additionally, the stability module calculates the one-engine-inoperative trim under the most unfavorable circumstances, using the method in Roskam.[9] The take-off rotation speed with the pitch control surfaces in take-off rotation deflection is calculated by considering the equilibrium situation.

2.3.6 Performance Module

With all necessary data known, the performance module refines the performance estimates. The cruise performance is evaluated by calculating the lift-to-drag ratio using aerodynamic data and trim drag from the trim and stability module. The range for each cruise flight phase is calculated, to construct the payload-range diagram. The take-off and landing distance are calculated using Raymer's balanced field length method.[8] The climb performance is calculated from the excess power at maximum continuous engine thrust at sea-level.

2.3.7 Constraints Module

The constraints module compares the calculated characteristics of the aircraft with top-level requirements and aviation regulations. The constraints are presented in Table 2.

Table 2 Constraints summary

Parameter	Constraints	Unit
Wing span	$b < 80$	m
Aircraft overall length	$l < 80$	m
Cabin floor area	$S_{\text{cabin}} \geq S_{\text{cabin}_{\text{req}}}$	m^2
Cargo volume	$V_{\text{cargo}} \geq V_{\text{cargo}_{\text{req}}}$	m^2
Take-off distance	$s_{\text{TO}} \leq s_{\text{TO}_{\text{req}}}$	m
Landing distance	$s_{\text{land}} \leq s_{\text{land}_{\text{req}}}$	m
Stall speed take-off	$V_{\text{stall}_{\text{TO}}} \leq V_{\text{stall,TO}_{\text{req}}}$	m/s
Stall speed clean	$V_{\text{stall}} \leq V_{\text{stall}_{\text{req}}}$	m/s
Climb gradient OEI1	$\gamma_{\text{OEI1}} > 0.012$	–
Climb gradient OEI2a	$\gamma_{\text{OEI2}a} > 0.000$	–
Climb gradient OEI2b	$\gamma_{\text{OEI2}b} > 0.000$	–
Climb gradient OEI2c	$\gamma_{\text{OEI2}c} > 0.012$	–
Climb gradient OEI3	$\gamma_{\text{OEI3}} > 0.032$	–
Climb gradient AOE1	$\gamma_{\text{AEO1}} > 0.021$	–
Maximum trim deflection	$\delta_h < 12$	deg
Minimum static margin	$\text{SM} > -10$	%
Directional stability	$C_{n_\beta} = 0.010$	–
Dihedral effect	$C_{l_\beta} < 0$	–
Take-off rotation speed	$V_{\text{rot}} < V_{\text{stall}_{\text{TO}}}$	m/s
Drag divergence Mach	$M_{\text{DD}} \leq M_{\text{cruise}}$	–
Nose wheel load	$0.05 < F_{\text{nlg}} < 0.20$	–
Nose landing gear position	$x_{\text{nlg}} > x_{\text{nose}} + 0.5$	m
Main landing gear position	$x_{\text{le}} < x_{\text{mlg}} < x_{\text{te}}$	m

3 Results and Discussion

By operating the MMG and subsequent analysis modules, the designer can almost instantly analyze a certain blended wing body configuration and compare it to the set of constraints of Table 2. This allows the designer to generate a number of different BWB configurations based on a set of 31 input parameters and a set of predefined airfoils and compare their respective performance in order to make a judgement on which design is most promising. Examples of various BWB configurations are presented in Figure 6. In addition, the input of the geometry module and the output of the analysis module is structured such that for a chosen configuration an optimizer can be employed to find a feasible (or even optimal) BWB geometry that fulfills all the top-level requirements and FAR/CS constraints. In the following subsections three examples are presented that are exemplary for the capability of the design tool.

The aircraft is designed to carry an equal payload of 400 passengers and 22,000 kg of freight. The maximum take-off weight of the three aircraft is equal, which allows an objective comparison based on cruise range, empty weight and constraints. The cruise speed is Mach 0.82 and the landing and take-off runway length should be less than 2,500 m. In the subsequent sections, three different BWB aircraft are designed for these requirements and sequently compared.

3.1 Example: Design of a 'Conventional' BWB

The most conventional BWB configuration from previous studies has aft-swept wings, two vertical tails at the wing tip (doubling as winglets), and the engines positioned close to the trailing edge of the center section (see Figure 10). When trying to find a solution for this configuration that satisfies all the constraints of Table 2, various constraints appear to be prohibitive. The most important aspect of this configuration are discussed in this section. The input parameters used to construct this concept are given in Figure 7.

Input vector

	Sect 1	Sect 2	Sect 3	Sect 4	Sect 5	Sect 6	
Chords	39.7	39.1	35.1	23.2	12	5.26	m
Spans		1.18	3.58	8.86	14.7	32.4	m
Twists					1.54	−0.777	°
Sweeps		17.6	57.6	48	48	48	°
Dihedral		0.606	−0.545	1.03	2.01	4.61	°
t/c	0.188	0.176	0.157	0.157	0.142	0.142	%
Tail h	8.67						m

Fig. 7 Conventional BWB configuration, aft mounted engines input

A summary of the most important performance and constraint parameters is given in Table 3 in Section 3.4. The wing area and wing loading of all three aircraft lie close to each other. The wing area of the 'conventional' BWB is 1091 m^2, which gives a wing loading of 3650 m/N^2. The empty weight of the aircraft is 190.4 10^3 kg, which is the highest of the three aircraft. The reason for this is the lift distribution, which gives a higher bending moment and causes a larger structural weight of the wing-body structure. Since the payload weight and the maximum take-off of all aircraft are equal, this leaves a smaller amount of fuel weight compared to the other concepts.

This concept has the highest lift-to-drag ratio. The maximum lift-to-drag ratio is 27.9, with an average lift-to-drag of 27.2 for a maximum-payload mission. This concept is aerodynamically very efficient. The cause is the favorable lift distribution and the presence of the winglets. The fuel consumption is 0.0207 kg/pax/km, which is 10% lower compared to the other concepts. The maximum-payload range is 14,359 km and the ferry range is 17,670 km. The main influences on the maximum-payload range are the fuel weight and the aerodynamic efficiency.

The 'conventional' BWB has the lowest maximum lift coefficients and consequently the longest take-off and landing distances. The lift distribution is unfavorable for low speed flight. Tip stall is likely to occur and the lift distribution is unfavorable for the maximum lift coefficient. The aircraft has a minimum static margin of -8.43%, which occurs when flying without payload and at maximum fuel weight. With these

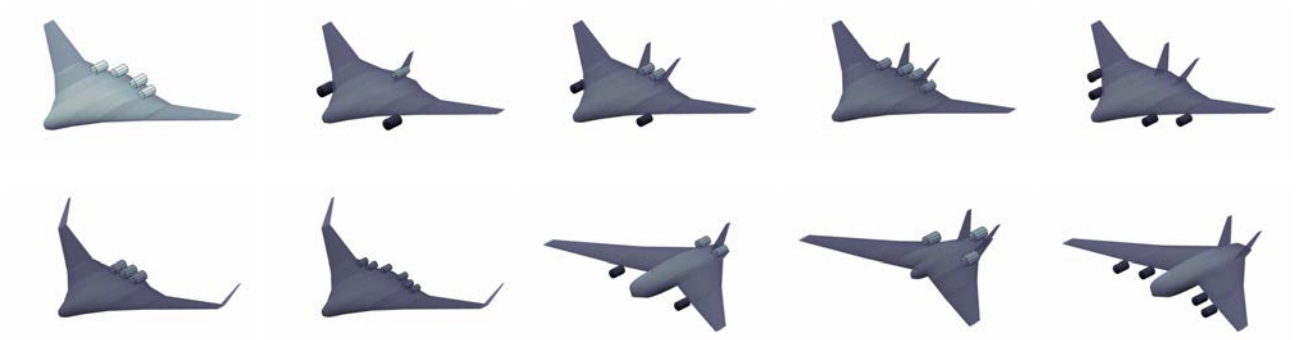

Fig. 6 Example of Various BWB Configurations Generated by the MMG

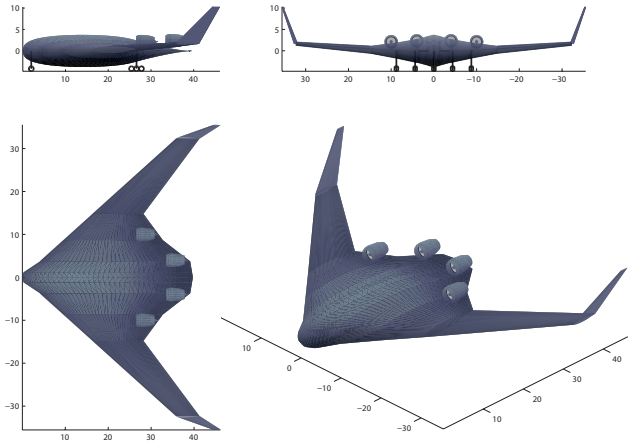

Fig. 8 Conventional BWB configuration, aft mounted engines

Input vector

	Sect 1	Sect 2	Sect 3	Sect 4	Sect 5	Sect 6	
Chords	40.1	39.4	34.7	23.2	13.4	3.62	m
Spans		1.01	3.3	8.4	13.3	32.1	m
Twists					3	2.53	°
Sweeps		28.6	64.7	47.7	46.2	46.2	°
Dihedral		0.348	−0.851	0.929	0.744	5	°
t/c	0.178	0.177	0.174	0.13	0.13	0.13	%
Tail h	8.03						m

Fig. 9 Conventional BWB configuration, wing mounted engines input

conditions the center of gravity is shifted far aft, causing the aircraft to be unstable. The aircraft turns out to be instable during most parts of the flight envelope. The shift in center of gravity expressed in terms of the MAC is the largest of the three concepts. This is mainly caused by the position of the fuel tanks relative to the payload and empty weight's center of gravity.

3.2 Example: Design of a BWB with wing-mounted engines

The second concept is very similar to the first concept. The input parameters used to construct this concept are given in Figure 9. The engine position is changed from aft mounted engines, to wing mounted engines. The reason for this is to investigate the effect of the engine position on the longitudinal stability of the aircraft. The previous concept showed a minimum static margin of -8.43%, while this concept has a minimum static margin of only -2.47%. Moreover, the concept turns out to have a positive static margin throughout most of the flight envelope. For a maximum-payload range mission, the aircraft is always stable. The only instability occurs during a ferry range mission, at the very start of the cruise flight, with almost full fuel tanks.

Compared to the previous concept, this concept has a lower lift-to-drag ratio. The maximum lift-to-drag ratio is 25.5 and the average lift-to-drag ratio in cruise flight is 23.7. The lower aerodynamic efficiency is caused by the lift distribution, leading to a 10% higher fuel consumption. The lift distribution tends to unload the wing tips. This, in turn, is favorable for the structural weight and low speed performance. The empty weight is 182.5 10^3 kg, which is smaller compared to the previous concept. The impact of the lower aerodynamic efficiency on the range is limited by the smaller empty weight. The smaller empty weight

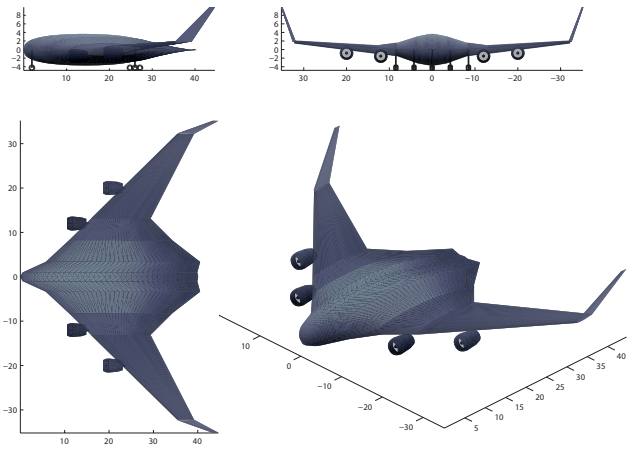

Fig. 10 Conventional BWB configuration, wing mounted engines

means that more fuel is available. The maximum-payload range is 13,599 km and the ferry range is 14,273 km. The latter is relatively small, because of the limited size of the fuel tanks. The maximum lift coefficients in clean and slats extended configuration are 1.47 and 1.63 which is considerably higher than the previous concept. The take-off and landing distances are smaller and are 1,673 m and 2,230 m, respectively.

The most notable aspect of this concepts are the nose load. The variation is very large and the nose loads are at the limits of 5% and 20% of the weight respectively. This is caused by the short-coupled nature of the Blended Wing Body. The nose landing gear is close to the nose, and cannot be moved forward to increase the margins of the nose loads. The rudder trim deflection in one-engine-out condition is much larger than the other two concepts, which due to the fact that the critical engine is located further outboard.

3.3 Example: Design of a Forward Swept BWB

A more unusual BWB configuration that has been analyzed is a forward-swept concept with engines hanging from pylons under the wing (see Figure 12). The input parameters used to define this concept are given in Figure 11. The forward sweep can exhibit considerable benefits in transonic flow, due to the increased shock-

Input vector

	Sect 1	Sect 2	Sect 3	Sect 4	Sect 5	Sect 6	
Chords	36.9	36.1	22.1	19.7	15	2.58	m
Spans		1.07	8.59	11.1	16.7	31.4	m
Twists					−0.228	4.02	°
Sweeps		29.5	64.6	−28.6	−28.6	−28.4	°
Dihedral		0.88	3.97	0.505	1.7	5	°
t/c	0.189	0.189	0.18	0.18	0.15	0.15	%
Tail h	8.34						m

Fig. 11 Forward-Swept BWB configuration input

wave sweep, the reduction of tip-stall tendencies, and successful implementation of natural laminar flow technology.[13] Even though none of these effects can be quantified in the conceptual design stage, it is of interest to see if such a configuration could meet the constraints of Table 2. The engines are located beneath the wing for longitudinal stability reasons. When using the same planform with the engines mounted on the aft-body, the aircraft turned out to have a minimum static margin of -47%, effectively ruling out this configuration.

From the planform the decreased leading edge sweep over the previous concept can be observed. This confirms the expectations that less leading edge sweep is required for forward-swept wing aircraft compared to aft-swept wing aircraft, to meet divergence Mach number requirements. The other most notable aspect is the very low operational empty weight. The operational empty weight is only $156.7 \cdot 10^3$ kg. Since the maximum take-off weight of the three concept is kept equal, the fuel weight is relatively large. This, in turn, means a very large range. The maximum-payload range is 16,452 km and the ferry range is 21,875 km. The aerodynamic efficiency is somewhat lower than the aft-swept wing concepts with the maximum lift-to-drag ratio being 23.7 and the average lift to drag ratio in cruise flight being 22.5. The fuel consumption is almost equal to the previous concept and is 0.0235 kg/pax/km.

The empty weight of the aircraft is small because of the lift distribution. The lift-distribution is is also favorable at low speed conditions. Stall is likely to occur on the inboard parts of the

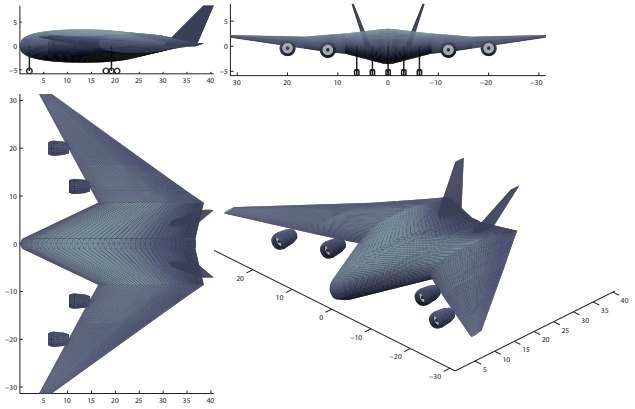

Fig. 12 Forward-Swept BWB configuration

wings and the maximum lift coefficient is relatively high. The maximum lift coefficients in clean and slats extended configuration are 1.44 and 1.58 respectively, which is close to the values of the previously discussed concept. The take-off and landing distances are similar as well.

The minimum static margin lies in between the previous two concepts and has a value of -5.54%. Since the fuel's center of gravity, the payload's center of gravity and the empty weight's center of gravity are located close to each other the center of gravity travel is small compared to the aft-swept wing concepts. The center of gravity travel is only 9.41% of the MAC. This also means that the trim variation is less and therefore the maximum trim deflection is less than one degree. The size of the control surface may be reduced for this type of configuration.

3.4 Concept Comparison

In Table 3 the results of the optimized aircraft are displayed. Values printed in blue highlight the best values, while values printed in red highlight the worst values.

Parameter	Symbol				Unit
Wing area	S	1091	1043	1074	m^2
Wing span	b	64.9	64.4	62.7	m
Aspect ratio	A	3.86	3.98	3.67	-
Wing loading MTOW	W/S	3650	3818	3706	N/m^2
Overall length	-	41.4	40.5	38.5	m
MTOW	W_{TO}	405.9	405.9	405.8	10^3 kg
OEW	W_{OE}	190.4	182.5	156.7	10^3 kg
Payload weight	W_{pl}	66.4	66.4	66.4	10^3 kg
Fuel weight	W_f	149.1	157.0	182.7	10^3 kg
Max-payload range	R_{maxpl}	14359	13599	16452	km
Ferry range	R_{ferry}	17670	14273	21875	km
Fuel consumption	-	0.0207	0.0234	0.0235	kg/pax/km
Max lift-to-drag ratio	$(L/D)_{max}$	27.9	25.5	23.7	-
Av lift-to-drag ratio	$(L/D)_{av}$	27.2	23.7	22.5	-
Max lift coefficient	$C_{L_{max,clean}}$	1.12	1.47	1.44	-
Max lift coeff, slats	$C_{L_{max,land}}$	1.28	1.63	1.58	-
CG travel	-	14.9	13.6	9.41	% MAC
Cabin floor area	S_{cabin}	312	276	273	m^2
Cargo volume	V_{cargo}	186	216	239	m^3
Take-off distance	s_{TO}	2006	1673	1655	m
Landing distance	s_{land}	2477	2230	2249	m
Stall speed TO land	$V_{stall_{TO}}$	62.6	56.6	56.7	m/s
Stall speed clean	V_{stall}	66.7	59.7	59.3	m/s
Climb gradient OEI1	γ_{OEI1}	7.4	5.5	5.0	%
Climb gradient OEI2a	γ_{OEI2a}	4.0	2.0	1.4	%
Climb gradient OEI2b	γ_{OEI2b}	7.4	5.5	5.0	%
Climb gradient OEI2c	γ_{OEI2c}	10.6	8.7	8.3	%
Climb gradient OEI3	γ_{OEI3}	17.0	16.7	16.4	%
Climb gradient AOE1	γ_{AEO1}	16.6	15.6	15.1	%
Max trim deflection	$\delta_{e,max}$	4.5	4.8	0.9	deg
Min static margin	SM	-8.43	-2.47	-5.54	% MAC
Weathercock stability	C_{n_β}	0.0524	0.0311	0.0747	1/rad
Effective dihedral	C_{l_β}	-0.138	-0.100	-0.0329	1/rad
Take-off rotation speed	V_{rot}	30.8	31.1	27.1	m/s
OEI rudder deflection	$\delta_{r,OEI}$	6.24	21.2	8.41	deg
Drag div Mach out tr	M_{DD}	0.93	0.90	0.84	-
Drag div Mach out tr-1	M_{DD}	0.82	0.82	0.82	-
Nose landing gear x	x_{nlg}	1.99	1.90	1.99	m
Main landing gear x	x_{mlg}	26.9	26.0	19.2	m
Minimum nose load	-	6.3	5.0	8.5	%
Maximum nose load	-	18.7	20.0	16.5	%

Table 3 Concept comparison table

4 Conclusion and Future Work

A conceptual design tool for the configuration design of a blended wing body (BWB) has been presented. The capability of this tool allows the designer to quickly alter the main geometric components of the airplane and analyze its effect on key characteristics such as flight and field performance, static stability, balance, weight, and passenger accommodation. The tool includes methods for the sizing of all components (body, wing, fin, landing gear) relevant to this design stage and relies on modified handbook methods for BWB-specific components, such as the structural layout of the cabin, the structural weight estimation and aerodynamic analysis of the aircraft.

Future work includes the refinement of various analysis methods, tailored to increase the fidelity of the analysis modules. The present work is to be integrated in a conceptual design and analysis tool that allows the designer to generate conventional and nontraditional airplane configurations such as a box-wing configuration and a blended-wing-body configuration. Finally, this tool is to become the first part in a rule-based de-

sign framework in which the fidelity of the geometric and analysis models increases progressively with each design step.[14] The robust implementation of the present work within this framework is the subject of future investigations.

Acknowledgements

The authors would like to thank Dr. E. Torenbeek for sharing his insights on non-conventional airplane configurations and introduction to relevant literature.

References

[1] Denning, R., Allen, J., and Armstrong, F., "The broad delta airliner," *The Aeronautical Journal*, Vol. 107, No. 1075, September 2003, pp. 547–558.

[2] Liebeck, R., "Design of the Blended Wing Body Subsonic Transport," *Journal of aircraft*, Vol. 41, 2004, pp. 10 – 25.

[3] Hileman, J. I., Spakovszky, Z. S., Drela, M., Sargeant, M. A., and Jones, A., "Airframe Design for Silent Fuel-Efficient Aircraft," *Journal of aircraft*, Vol. 47, 2010, pp. 956 – 970.

[4] van Dommelen, J. L., "Design of a Forward-Swept Blended Wing Body Aircraft," Tech. rep., Delft University of Technology, Oct. 2011.

[5] Roskam, J., *Airplane design, Part I: Preliminary sizing of airplanes*, The University of Kansas, 1990.

[6] Roskam, J., *Airplane Design Part I: Preliminary Sizing of Aircraft*, DARcorp, Lawrence, KS, 2005.

[7] Morris, A. J., "MOB A European Distributed Multi-Disciplinary Design and Optimisation Project," Tech. Rep. AIAA 2002-5444, Cranfield University, Sep. 2002.

[8] Raymer, D., *Aircraft design: A conceptual approach*, American Institute of Aeronautics and Astronautics, Inc, 2006.

[9] Roskam, J., *Airplane design, Part VI: Preliminary calculation of aerodynamic, thust and power characteristics*, The University of Kansas, 1990.

[10] Kroo, I., *Aircraft design, Synthesis and Analysis*, Desktop Aeronautics, Inc, Jan 2001.

[11] Torenbeek, E., "Development and Application of a Comprehensive, Design-sensitive Weight Prediction Method for Wing Structures of Transport Category Aircraft," Tech. rep., Delft University of Technology, Department of Aerospace Engineering, 1992.

[12] F. J. J. M. M. Geuskens, O. K. Bergsma, S. K. and Beukers, A., "Analysis of Conformable Pressure Vessels: Introducing the Multibubble," Tech. Rep. AIAA 54561-869, Delft University of Technology, Aug. 2011.

[13] Obert, E., *Aerodynamic design of transport aircraft lecture notes*, Delft University of Technology, 2007.

[14] Rocca, G. L., Langen, T., and Brouwers, Y., "The Design and Engineering Engine: Towards a Modular System for Collaborative Aircraft Design (accepted)," ICAS 2012, Brisbane, Australia, September 2012.

Nomenclature

b	Wing span, m
c	Chord, m
C_{n_β}	Weathercock stability, 1/rad
C_{l_β}	Effective dihedral, 1/rad
$C_{l_{\max}}$	Maximum lift coefficient, -
M_{cruise}	Cruise Mach number, -
l	Aircraft overall length, m
L/D	Lift-to-drag ratio, -
s	Runway length, m
S_{cabin}	Cabin floor area, m^2
V_{cargo}	Cargo volume, m^3
V_{rot}	Take-off rotation speed, m/s
V_{stall}	Stall speed, m/s
W_{f}	Fuel weight, kg
W_{OE}	Operational empty weight, kg
W_{pl}	Payload weight, kg
W_{TO}	Take-off weight, kg
x	Aircraft x-position, m
δ	Control surface deflection, deg
ε	Wing twist, deg
γ	Climb gradient, %
Γ	Wing dihedral, deg
Λ	Wing sweep, deg

Subscripts

0	zero altitude
clean	clean configuration
land	landing
TO	take-off

Abbreviations

BWB	Blended Wing Body
CS	Certification Specification
DD	drag divergence
FAR	Federal Aviation Regulations
le	leading edge
MAC	Mean aerodynamic chord
mlg	main landing gear
nlg	nose landing gear
OEI	one engine inoperative
SM	static margin
TAW	Tube and Wing Aircraft
te	trailing edge
TO	take-off